Kalman-filter-based control for adaptive optics

Cyril Petit, Fernando Quiros-Pacheco, Jean-Marc Conan, Caroline Kulcsar, Henri-Francois Raynaud, et al.

Cyril Petit, Fernando Quiros-Pacheco, Jean-Marc Conan, Caroline Kulcsar, Henri-Francois Raynaud, Thierry Fusco, Gerard Rousset, "Kalman-filter-based control for adaptive optics," Proc. SPIE 5490, Advancements in Adaptive Optics, (25 October 2004); doi: 10.1117/12.550775

SPIE.

Event: SPIE Astronomical Telescopes + Instrumentation, 2004, Glasgow, United Kingdom

Kalman filter based control for Adaptive Optics

C. Petit[a], F. Quiros-Pacheco[b], J.-M. Conan[a], C. Kulcsár[c], H.-F. Raynaud[c], T. Fusco[a], and G. Rousset[a]

[a]ONERA, BP 72, 92322 Châtillon, France
[b]Imperial College, London, UK
[c]Université Paris 13, Institut Galilée, L2TI, 93430 Villetaneuse, France

ABSTRACT

While the first MultiConjugate Adaptive Optics (MCAO) experimental set-ups are presently under construction, a growing attention is paid to the control loop. This is indeed a key element in the optimization process, especially for MCAO systems. Different approaches have been proposed in recent articles for astronomical applications: simple integrator, Optimized Modal Gain Integrator and Kalman filtering. We study here Kalman filtering, which seems a very promising solution.

We have already proposed and simulated in simple cases a formalized adaptation of Kalman filtering to Adaptive Optics (AO) and MCAO .[1–3] We wish now to characterize for the first time the frequential properties of this Kalman filter and to refine it so as to improve its robustness and performance, for instance in the presence of static aberrations and vibrations. Comparisons with classical controllers are proposed. Aliasing reduction could also be considered. In the near future, Kalman filter performance and robustness should be tested for realistic AO and MCAO configurations on a simulator and an experimental set-up.

Keywords: MultiConjugate Adaptive Optics, Kalman filter, transfer functions, static aberrations, vibrations

1. INTRODUCTION

For a few decades, Adaptive Optics (AO) systems have proved their efficiency for high resolution imaging with ground based telescopes, hence equipping a growing number of them. In the meantime, MultiConjugate Adaptive Optics (MCAO) has remained merely a theoretical concept designed to compensate for their limitation of the corrected Field of View (FoV), due to anisoplanatism. In this approach, several Wave-Front Sensors (WFSs) looking at different Guide Stars (GSs) are used to control several Deformable Mirrors (DMs) optically conjugated at different altitudes. A large FoV correction can be thus obtained.[4] The first experimental set-ups are now under construction.[5–9] Henceforth, as for AO systems, the issue of reconstruction and control has drawn much attention recently.[2,10–14]

Optimal AO reconstruction, in terms of minimum mean square error, exists[15] but has a high computational cost and most of all is hardly adapted to closed-loop systems. Hence, the classical AO systems are sub-optimal and based on integrator or Optimized Modal Gain Integrator (OMGI).[16,17] Although no global optimization is done, that does not prevent these AO systems to achieve good performance. But in the case of MCAO, it has been demonstrated[3,18] that unseen modes and badly seen modes must be well estimated to ensure a good and stable reconstruction of the turbulence in the FoV. Classical approaches are no more efficient. It has been already shown[15] that open-loop MCAO finds an optimal reconstruction solution in Minimum Mean Square Estimation (MMSE) as for open-loop AO optimal reconstruction, taking into account spatial priors on the volumic turbulence, as well as information on the measurement noise. Unseen modes can be then managed. But closing the loop brings a considerable amount of new difficulties among which time delay, stability and robustness management.

These are the reasons that lead first Paschall and Anderson,[19] and then B. Le Roux et al.[1] to introduce Kalman filtering in MCAO systems. B. Le Roux has shown first in AO then in MCAO systems the significant gain brought by a Kalman filter, which ensures an optimal control law and stability, also accounting for the system properties (noise, direction of measurements and correction, number of wavefront sensors and Deformable Mirrors, time delay, etc). In an AO system

Further author information: (Send correspondence to Petit Cyril)
Petit Cyril: E-mail: cyril.petit@onera.fr

Advancements in Adaptive Optics, edited by Domenico Bonaccini Calia, Brent L. Ellerbroek, Roberto Ragazzoni, Proceedings of SPIE Vol. 5490 (SPIE, Bellingham, WA, 2004)
0277-786X/04/$15 · doi: 10.1117/12.550775

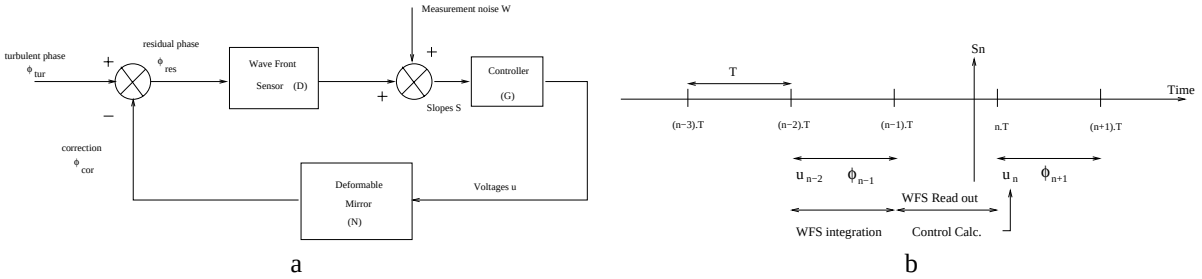

Figure 1. a) bloc diagram of AO closed-loop. b) temporal diagram of the system process.

the gain is lower and mainly due to temporal priors and prediction.[2] But it could be useful in eXtreme AO (XAO) and for Extremely Large Telescopes (ELT).

In this paper, we focus on a simplified closed-loop AO system as presented in Sect. 2. This simplification allows us to isolate given problematics and properties and to refine our models used as system description priors, so as to improve the performance of the Kalman filter. In the meantime, it also reveals the consequences of model errors. In the future, the methods described here should be extended to MCAO systems without much further complications. We propose to characterize first some properties of the Kalman filter in terms of transfer functions in Sect. 3. It is indeed possible to estimate in some extent modal transfer functions, which allows a comparison with classical controllers such as Optimized Modal Gain Integrator. It also gives much information about the frequential behavior of the Kalman filter. Finally, it appears that a rather straightforward modification of the system model could allow static aberration and vibration filtering as suggested in.[1] Here we propose in Sect. 4 and Sect. 5 a real implementation and first results. All these issues are tackled analytically first and then tested thanks to a proprietary simulator of an end-to-end AO/MCAO system in a discrete-time approach.

2. AO AND KALMAN FILTER: NOTATIONS AND BASIC EQUATIONS

We describe here our implementation of the Kalman filter. As previously announced, we will focus only on its AO version. Notations and equations, largely inspired from,[1,2] will thus be simplified. Sect. 2.1 presents the system while Sect. 2.2.1 introduces the optimal control law problematic and the priors used in Sect. 2.2.2 to describe the closed-loop AO Kalman filter. Finally, Sect. 2.3 is dedicated to our simulator and its main parameters.

2.1. System Description

We consider in this article an AO system, based on a single WFS and single DM, used in a closed-loop configuration (see Fig. 1 a). WFS and DM are supposed to be linear. Dealing with a closed-loop system, temporal considerations are important. We assume that measurements are obtained with an exposure time T, corresponding to CCD integration. CCD read out and voltages computation are done during a same time period T. We also consider that the DM reacts very fast compared to the sampling period so that we can neglect its dynamics. This assumption is generally valid for the current AO systems using piezo-stacked DM and operating at a few hundred Hertz. Accounting for DM dynamics is possible particularly with a Kalman filter but will not be discussed here. The correction is then constant during a sampling period T.

As a consequence, our system has both a continuous part (the incoming signal) and a discrete part (measurement and correction). But as explained in,[3] the optimal correction of a continuous signal $x(t)$, in term of minimum mean square, by a command constant over a sampling period T with no dynamics, is the average of the signal over the period, x_n:

$$x_n = \frac{1}{T}\int_{(n-1)T}^{nT} x(t)dt. \tag{1}$$

Thus, considering our model of command and measurement, our optimal control law problem is equivalent when considering as input signal the discretized turbulent phase defined as in Eq. (1).

Figure 1 b) shows then the succession of operations in this discretized approach: the incoming turbulent phase is integrated by the detector during the frame delay $[(n-2)T,(n-1)T]$ and is so noted ϕ^{tur}_{n-1}. The correction phase ϕ^{cor}_{n-1} is generated instantaneously and continuously during the frame delay $[(n-2)T,(n-1)T]$ by the DM when the voltages $\mathbf{u}_{n-2}$ are applied. The matrix $\mathbf{N}$ defining the relationship between voltages and the generated correction phase is the so-called influence matrix. Thus:

$$\phi^{cor}_{n-1} = \mathbf{N}\mathbf{u}_{n-2}. \tag{2}$$

As a result, the WFS measurement process can be modeled through the equation:

$$\mathbf{S}_n = \mathbf{D}\phi^{res}_{n-1} + \mathbf{W}_n, \tag{3}$$

where ϕ^{res}_{n-1} is the residual phase defined as $\phi^{res}_{n-1} = \phi^{tur}_{n-1} - \phi^{cor}_{n-1}$, $\mathbf{S}_n$ is the vector containing all the slopes measurements, $\mathbf{D}$ is the interaction matrix of the WFS describing the relationship between the phase and the measurement. Finally, $\mathbf{W}_n$ is the measurement white noise of covariance matrix $\mathbf{C}_w$. $\mathbf{S}_n$ is obtained during the frame period $[(n-1)T,nT]$, after CCD read out, and is used to compute the next correction applied through the voltages $\mathbf{u}_n$ to correct for the turbulent phase integrated during the next frame delay $[nT,(n+1)T]$, ϕ^{tur}_{n+1}. This is then a two-frame delay system.

2.2. Optimal Reconstruction and Control

2.2.1. Global framework

We can now define an optimal correction criterion. It corresponds to the voltages $\mathbf{u}_n$ that minimize the mean square error defined as:

$$\varepsilon_{n+1} = \left\langle \left\| \phi^{tur}_{n+1} - \phi^{cor}_{n+1} \right\|^2 \right\rangle_{\phi,noise} = \left\langle \left\| \phi^{tur}_{n+1} - \mathbf{N}\mathbf{u}_n \right\|^2 \right\rangle_{\phi,noise}, \tag{4}$$

where $\|\phi\|^2 = \frac{1}{S}\int_S \phi(\mathbf{r})^2 d\mathbf{r} = \sum_i \phi_i^2$ if the base is orthonormalized, denotes the so called spatial variance in the telescope pupil S and $\langle . \rangle_{\varphi,noise}$ stands for average over turbulence and noise outcomes.

It has been noted [1,20,21] that finding the optimal solution of Eq. (4) can be split into first a stochastique estimation problem and then a deterministic control problem. This is indeed a special case of the famous separation theorem established in the 1960s' in optimal stochastic control theory, [22] which states that the minimum-variance control for linear system with additive gaussian noise is obtained by combining an optimal deterministic control (LQ state feedback) with an independently constructed optimal estimator (Kalman filter). The first problem is thus to estimate the turbulent phase minimizing a stochastic criterion ε^1_{n+1}:

$$\varepsilon^1_{n+1} = \left\langle \left\| \phi^{tur}_{n+1} - \hat{\phi}^{tur}_{n+1} \right\|^2 \right\rangle_{\phi,noise}. \tag{5}$$

The Kalman filter provides this solution. The second one is to find the best commands of the DM, $\mathbf{u}_n$, minimizing ε^2_{n+1}:

$$\varepsilon^2_{n+1} = \left\| \hat{\phi}^{tur}_{n+1} - \mathbf{N}\mathbf{u}_n \right\|^2. \tag{6}$$

It is then a deterministic problem whose solution is given by the projection of $\hat{\phi}^{tur}_{n+1}$ on the DM modes.

While the second problem is rather straightforward, the first one implies, as well as in an open-loop optimal reconstruction, to take into account prior knowledge on the turbulence and global noise. We will use the same priors as, [1] that means the turbulence evolution can be described by:

$$\phi^{tur}_{n+1} = \mathbf{F}\left[\phi^{tur}_n, \phi^{tur}_{n-1}, \phi^{tur}_{n-2}, ...\right] + \nu_n, \tag{7}$$

where ν is a white noise, of covariance matrix $\mathbf{C}_\nu$, and $\mathbf{F}$ is a linear function. And the same first order model approximation will be used to simplify this equation:

$$\phi^{tur}_{n+1} = \mathbf{A}\phi^{tur}_n + \nu_n. \tag{8}$$

Matrix $\mathbf{A}$ is defined as in,[1] thanks to the modal cut-off frequencies of the Power Spectral Densities (PSD) of a Taylor turbulent phase described on a Zernike basis. $\mathbf{A}$ defines the temporal correlation of the phase. Ensuring the conservation of the global energy of the turbulence then leads to:

$$\mathbf{C}_v = \mathbf{C}_\phi - \mathbf{A}^T \mathbf{C}_\phi \mathbf{A}, \tag{9}$$

with $\mathbf{C}_\phi$ the covariance matrix of the turbulent phase. Thus, the spatial and temporal priors on the turbulence are described by choosing $\mathbf{C}_\phi$ and $\mathbf{A}$ respectively which imposes $\mathbf{C}_v$. As discussed in,[1] this first order approach of the temporal correlation of the turbulence is simple but it only aims at describing the correlation of the turbulence at one or two steps and not the full physical process.

2.2.2. Optimal estimation: Kalman filter basic equations

We now recall the Kalman filter basic equations giving the solution of Eq. (5). In the following **Id** is the identity matrix. It is important to bear in mind that the idea of a Kalman filter is to use the full system description and the prior knowledge we have on it. It is formalised using state vectors gathering the components that give a full description of the system. In our case, the system is completely defined by the turbulent phase at different moments and the commands applied. Additional information is brought by the measurements. Thus, with the system and the priors chosen previously, a convenient choice of state vector is:

$$\mathbf{X}_n = \begin{pmatrix} \phi^{tur}_{n+1} \\ \phi^{tur}_{n} \\ \phi^{tur}_{n-1} \\ \mathbf{u}_{n-1} \\ \mathbf{u}_{n-2} \end{pmatrix}, \tag{10}$$

and the state model equations are:

$$\mathbf{X}_{n+1} = \begin{pmatrix} \mathbf{A}_{tur} & 0 & 0 & 0 & 0 \\ \mathbf{Id} & 0 & 0 & 0 & 0 \\ 0 & \mathbf{Id} & 0 & 0 & 0 \\ 0 & 0 & 0 & 0 & 0 \\ 0 & 0 & 0 & \mathbf{Id} & 0 \end{pmatrix} \mathbf{X}_n + \begin{pmatrix} 0 \\ 0 \\ 0 \\ \mathbf{Id} \\ 0 \end{pmatrix} \mathbf{u}_n + \begin{pmatrix} \mathbf{Id} \\ 0 \\ 0 \\ 0 \\ 0 \end{pmatrix} v_{n+1}, \tag{11}$$

$$\mathbf{S}_n = \mathbf{D} \begin{pmatrix} 0 & 0 & \mathbf{Id} & 0 & -\mathbf{N} \end{pmatrix} \mathbf{X}_n + \mathbf{W}_n, \tag{12}$$

written in standard compact form as:

$$\mathbf{X}_{n+1} = A\mathbf{X}_n + B\mathbf{u}_n + \mathbf{V}_{n+1}, \tag{13}$$

$$\mathbf{S}_n = C\mathbf{X}_n + \mathbf{W}_n. \tag{14}$$

First Eq. (11) is simply the equation of evolution given in Eq. (8), the second one is the measurement Eq. (3). Once the system is fully described, the standard linear optimal filtering theory gives the optimal estimation of $\mathbf{X}_n$ minimizing the criterion of Eq. (5):

$$\hat{\mathbf{X}}_{n/n} = \hat{\mathbf{X}}_{n/n-1} + \mathbf{H}_n(\mathbf{S}_n - C\hat{\mathbf{X}}_{n/n-1}), \tag{15}$$

where $\hat{\mathbf{X}}_{n/n}$ is the estimation of $\mathbf{X}_n$ using $\{\mathbf{S}_0, ..., \mathbf{S}_n\}$ and priors. $\mathbf{H}_n$ is the observator gain and is doing the trade-off between model-based prediction and measurements. We can also deduce the associated recursive equation that will be in fact implemented in a simulator or real calculator:

$$\hat{\mathbf{X}}_{n+1/n} = A\hat{\mathbf{X}}_{n/n-1} + B\mathbf{u}_n + A\mathbf{H}_n(\mathbf{S}_n - C\hat{\mathbf{X}}_{n/n-1}), \tag{16}$$

where $\hat{\mathbf{X}}_{n+1/n}$ is the prediction of $\mathbf{X}_{n+1}$ using the measurements acquired till n and the priors. $\mathbf{H}_n$ is defined as:

$$\mathbf{H}_n = \mathbf{C}_{n/n-1} C^T \left(C\mathbf{C}_{n/n-1} C^T + \mathbf{C}_w \right)^{-1}, \tag{17}$$

with $\mathbf{C}_w$ the covariance matrix of the noise and $\mathbf{C}_{n/n-1}$ the covariance matrix of the state vector estimation error. $\mathbf{C}_{n/n-1}$ is computed by solving the Ricatti equation[23]:

$$\mathbf{C}_{n+1/n} = A\mathbf{C}_{n/n-1}A^T + \mathbf{C}_v - A\mathbf{C}_{n/n-1}C^T \left(C\mathbf{C}_{n/n-1}C^T + \mathbf{C}_w \right)^{-1} C\mathbf{C}_{n/n-1}A^T. \tag{18}$$

As this equation is independent from the data acquired during the closed-loop, it can be computed off-line, and approximated with the classical asymptotic solution.

2.2.3. Optimal control

Finally, once the optimal estimation has been computed, the optimal command must be found minimizing Eq. (6). The solution is a projection of the estimated phase and the voltages to be applied are defined as:

$$\mathbf{u}_n = \mathbf{P}\hat{\phi}^{tur}_{n+1/n} = \mathbf{P}\begin{pmatrix} 0 & \mathbf{Id} & 0 & 0 & 0 \end{pmatrix}\hat{\mathbf{X}}_{n+1/n} = \mathbf{M}\hat{\mathbf{X}}_{n+1/n}, \tag{19}$$

where $\mathbf{P}$ is the projector of the phase on the DM basis.

The gain brought by this optimal control law over an OMGI or any other controller not achieving optimality has been emphasized in[1] both in AO and MCAO. We now introduce the simulation conditions used to obtain the results presented in this paper.

2.3. AO/MCAO Simulator Short Description

Simulations have been performed thanks to a proprietary end-to-end AO/MCAO system simulator. This simulator is based on a modular structure, emulating each element of a real system, including a multi-layer turbulence with Kolmogorov statistics and a given temporal evolution, different kinds of WFSs, DMs, and controllers (integrator, OMGI, or Kalman). In all the simulations performed here, we simulate an AO system with only one turbulent layer in the pupil which temporal evolution is the first order Auto-Regressive (AR) approximation of a Taylor evolution as described in Eq. (8), so as to avoid model errors on the turbulence priors. N^{turb}_{zern} Zernike modes are used to generate this turbulent phase using recursive Eq. (8). The WFS and DM are linear and perfect, meaning they measure and reconstruct directly and respectively N^{WFS}_{zern} and N^{DM}_{zern} Zernike modes, with propagated noise for the measurement process.

In all this paper we also assume that $N^{WFS}_{zern} = N^{DM}_{zern} = N^{turb}_{zern}$. All the Kalman filter computation will thus be done in the particular basis of Zernike modes. Note that voltages directly match the N^{DM}_{zern} Zernike coefficients of the corrected phase ϕ^{cor}_{n-1}. Matrices $\mathbf{D}$, $\mathbf{N}$ and $\mathbf{P}$ are consequently the identity and no projection of the estimated phase is needed, which simplifies the second part of the optimal control Eq. (6) and projection Eq. (19). Any other basis could have been used but the Zernike modes are well suited to describe the turbulent phase and its temporal and spatial properties. The WFS propagated measurement noise is also well known on these modes.[24] The two-frame delay is due to buffering.

The main numerical parameters are a telescope diameter of 8 meters, one turbulent layer located in the pupil is considered and D/r_0 is 9.18, wind velocity is $10m.s^{-1}$, the magnitude of the star is 14. The simulated WFS reading noise is 8 electrons for a sampling rate of 200 Hz. Correction, imaging and wave front sensing are performed at $2.2\mu m$. The full system equations described before in Sect. 2.2.2 could be implemented this way on our simulator, nevertheless a more computationally efficient form is used in the software.

3. KALMAN FILTER TRANSFER MATRIX

3.1. Rejection Transfer Matrix Computation

As we consider in this paper only discrete-time variables, we will use only transfer matrix (or function) defined thanks to z-transform. Thus the transfer matrix of the Kalman controller $\mathbf{G}(z)$ and the Rejection Transfer Matrix (RTM) $\mathbf{E}(z)$ are defined by:

$$\mathbf{u}(z) = \mathbf{G}(z)\mathbf{S}(z), \tag{20}$$

$$\phi^{res}(z) = \mathbf{E}(z)\phi^{tur}(z). \tag{21}$$

The OMGI, like other modal approaches assuming that modes are uncoupled, treats each mode of the turbulent phase individually. This leads to considering several mono-input/mono-output subsystems with individual transfer functions. This simplification cannot be done here with a Kalman filter *a priori*. Still, we can estimate the transfer matrix of the controller and thus, the RTM of the overall closed-loop system. In the following equations we replace $\mathbf{C}_{n+1/n}$ and $\mathbf{H}_{n+1/n}$ by their asymptotical values $\mathbf{C}_\infty$ and $\mathbf{H}_\infty$. Taking the z-transform of Eq. (16), Eq. (19), we obtain (dropping the arguments of the time variable z from now on for simplification):

$$z\hat{\mathbf{X}}_{n/n-1} = A\hat{\mathbf{X}}_{n/n-1} + B\mathbf{u}_n + A\mathbf{H}_\infty(\mathbf{S_n} - C\hat{\mathbf{X}}_{n/n-1}), \tag{22}$$

$$\mathbf{u}_n = z\mathbf{M}\hat{\mathbf{X}}_{n/n-1}. \tag{23}$$

After a simple calculation one obtains the relationship between the input variable $\mathbf{S}_n$ and the controller output $\mathbf{u}_n$:

$$\mathbf{G}(z) = \mathbf{M}(\mathbf{Id} - z^{-1}A - B\mathbf{M} + z^{-1}A\mathbf{H}_\infty C)^{-1}A\mathbf{H}_\infty. \tag{24}$$

Then the RTM of the Kalman system is:

$$\mathbf{E}(z) = (\mathbf{Id} + z^{-2}\mathbf{N}\mathbf{G}(z)\mathbf{D})^{-1}. \tag{25}$$

For comparison, the transfer function $\mathbf{G}_{int}^{i}$ of an integrator controller of gain g^i on mode i (assuming all modes are uncoupled) is:

$$\mathbf{G}_{int}^{i} = \frac{g^i}{1 - z^{-1}} M_{rec}^{i}, \tag{26}$$

where M_{rec}^{i} is the reconstruction and projection matrix that associates amplitude on mode i to a given measurement slope vector.

These discrete time transfer matrices $\mathbf{G}$ and $\mathbf{E}$ are sparse and approximatively diagonal, as all the matrices used in our simplified AO models are diagonal, save the covariance matrix of the turbulent phase, which is quasi-diagonal. This is verified by numerical computation of the matrices. This allows us to consider uncoupled modes and modal transfer functions rather than transfer matrices. This is also all the more true as we consider high frequencies (a few Hertz is enough actually). Each transfer function $\mathbf{G}_i$ or rejection transfer function $\mathbf{E}_i$ is the i^{th} diagonal element of the corresponding matrix which simplifies greatly the estimation of the transfer functions from the simulation data. We shall be able then to analyse and compare Kalman transfer functions with any other controller transfer functions, for instance OMGI's.

3.2. Rejection Transfer Functions Analysis and Kalman Performance - Comparison with OMGI

Thanks to Eq. (25), and assuming modes were uncoupled, transfer functions can be numerically computed, analysed and compared with those of an OMGI for instance.

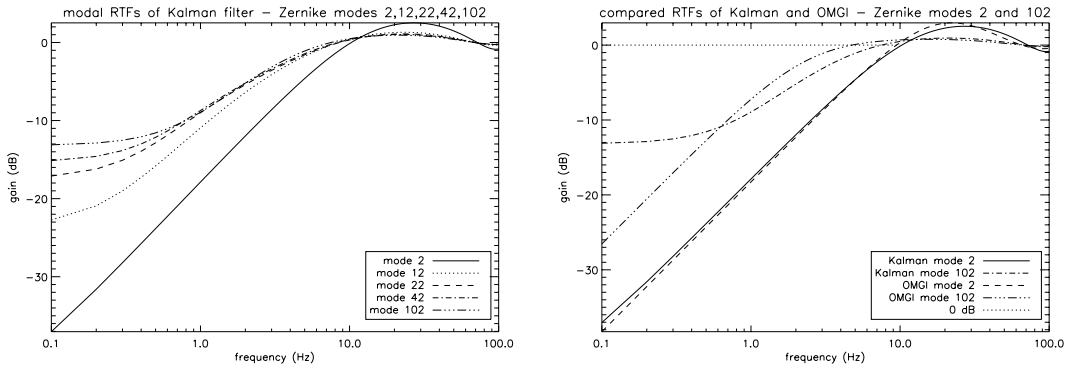

a) b)

Figure 2. a) Modal RTFs of Kalman filter. b) Comparison between Kalman and OMGI RTFs for Zernike modes 2 and 102.

Figure 2 a) proposes several RTFs of Kalman filter and a comparison with OMGI RTFs for 2 modes is proposed on Fig. 2 b). The transfer functions main outline is close to an integrator transfer function, with an overshoot at high frequency (this overshoot always exists and is directly related to the Bode theorem). But looking closer, many differences appear. First, each mode has a different RTF as seen on Fig. 2 a), with its own bandwidth and overshoot. A parallel could then be drawn with optimized modal integrator, as long as we consider that modes are uncoupled in the Kalman approach (only true here). This is not surprising as the Kalman filter optimizes the response, and following our assumption of uncoupled modes, the optimization is modal. But the main differences occur at low frequencies. Thus, the gain at low frequencies tends to a fixed value contrary to the integrator for which the RTF tends to infinity (with a classical 20dB/decade slope). This value is given by Eq. (25) when $z = 1$ and it depends on the SNR and the priors. Thus, it is all the higher (weak attenuation) as the the order of the mode is higher (see Fig. 2) a). We have also shown that this value for a given order increases with the noise (for a fixed value of signal i.e. SNR diminishes). The two cases are equivalent as the SNR

diminishes with the order of the mode. The second major difference between Kalman and OMGI occurs at poor SNR: the OMGI will be prone to associate a null gain with a poor SNR mode, or at least a very small gain and a very small bandwidth RTF. For instance, each controller modal bandwidth can be indeed estimated on Fig. 2 b) at the $0dB$ cut-off frequency: as we can see, as soon as the gain decreases for OMGI (mode 2: gain is 0.25, mode 102: gain is 0.066), the OMGI modal bandwidth becomes lower than the Kalman filter's one. The Kalman modal bandwidth is larger thanks to optimal control, and there is no 20dB/decade slope close to the 0 Hz frequency.

This leads to the conclusion that slowly varying aberrations and most of all, static aberrations are filtered as long as the attenuation is strong enough at low frequencies. It depends on the mode order and SNR, but it also depends on the temporal prior specified: static or slowly varying aberrations are all the more filtered as the temporal evolution of the turbulence is rather slow. Then the temporal prior and the temporal evolution of the aberrations are close, and the Kalman filter is able to attenuate the aberration just as the turbulent phase considering dynamics are close. So it could be interesting to refine our model to account for these aberrations when the attenuation at low frequencies is not strong enough (SNR is low and/or aberrations and turbulence dynamics are highly different). A slight modification of the Kalman filter model allows us to account for these aberrations and filter them.

As already shown in,[1] Kalman filter provides an improvement of the strehl ratio or the encircled energy in an AO system. As long as the priors are reasonable, the optimality of this controller ensures an minimum mean square error and better performance. For instance, in the given conditions of simulation, the mean strehl ratio measured on 2000 short exposure images is about 39.5% with Kalman filter, 35.5% with a 0.2 gain integrator, and 36.7% with OMGI. Note that when wind velocity increases or sampling rate decreases this performance of Kalman filter improve much more thanks to prediction.

4. STATIC ABERRATIONS FILTERING

4.1. Static Aberration Model and Kalman Filter Modification

It can be useful to filter static aberrations when we know there may be some in the system, which is usually true. Introducing static aberrations in our model is equivalent with refining the priors so as to account for another reality of the system. It is rather simple to adapt the previous model to filter static aberrations. Considering that the global phase seen by the system is the sum of a turbulent phase and static phase, the state vector is modified in:

$$\mathbf{X}_n = \begin{pmatrix} \phi^{stat}_{n+1} \\ \phi^{tur}_{n+1} \\ \phi^{tot}_{n} \\ \phi^{tot}_{n-1} \\ \mathbf{u}_{n-1} \\ \mathbf{u}_{n-2} \end{pmatrix}, \tag{27}$$

where $\phi^{tot}_n = \phi^{tur}_n + \phi^{stat}_n$. The prior on static aberrations is only a temporal prior: it is constant ! So that $\phi^{stat}_{n+1} = \phi^{stat}_n$. The new equations for the state-space model are then:

$$\mathbf{X}^{(1)}_{n+1} = \begin{pmatrix} \mathbf{Id} & 0 & 0 & 0 & 0 & 0 \\ 0 & \mathbf{A}_{tur} & 0 & 0 & 0 & 0 \\ \mathbf{Id} & \mathbf{Id} & 0 & 0 & 0 & 0 \\ 0 & 0 & \mathbf{Id} & 0 & 0 & 0 \\ 0 & 0 & 0 & 0 & 0 & 0 \\ 0 & 0 & 0 & 0 & \mathbf{Id} & 0 \end{pmatrix} \mathbf{X}_n + \begin{pmatrix} 0 \\ 0 \\ 0 \\ 0 \\ \mathbf{Id} \\ 0 \end{pmatrix} \mathbf{u}_n + \begin{pmatrix} 0 \\ \mathbf{Id} \\ 0 \\ 0 \\ 0 \\ 0 \end{pmatrix} v_{n+1}, \tag{28}$$

$$\mathbf{S}_n = \begin{pmatrix} 0 & 0 & 0 & \mathbf{D} & 0 & -\mathbf{DN} \end{pmatrix} \mathbf{X}_n + \mathbf{W}_n. \tag{29}$$

Matrices A, B, C have just to be modified in Eq. (13) and Eq. (14), and the associated matrices $\mathbf{C}_n$ and $\mathbf{H}_n$ must be computed taking into account this new model. The global method stays unchanged. This model improvement has only a slight computational cost.

4.2. Static Aberrations Filtering and Performance

Tests of static aberrations filtering have been performed on the simulator, in particular conditions: a worse SNR (star magnitude of 15, detector noise of 8 electrons), a higher wind speed ($20 m.s^{-1}$). As explained in Sect. 3.2 it may be necessary to filter static aberrations only in particularly bad conditions. In more common situations, taking static aberrations into account in the Kalman filtering is unnecessary. Static aberrations have been added on different modes (Zernike mode 4, 11, and 30). The priors, as explained before, just take into account the presence of aberrations of any value on any mode.

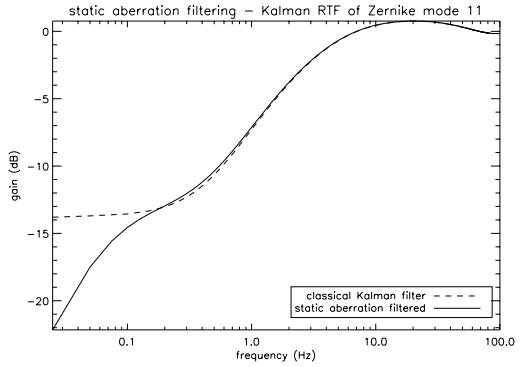

Figure 3. Kalman Rejection Transfer Function of Zernike mode 11, with and without static aberrations filtering.

As we can see on Fig. 3, the modified Kalman controller does filter the aberrations. The attenuation at very low frequencies is higher. It can be also shown that when the turbulence evolution is rather slow, the modified Kalman filter hardly estimates the static aberrations but on the overall they are corrected, because turbulence and aberration dynamics are close and both components are jointly estimated and corrected. With a faster turbulent evolution the estimation of the static aberrations is sharper. Of course, no comparison with Integrator or OMGI is needed here: static aberrations are completely filtered by these controllers.

To summarize, static aberrations are naturally filtered by the basic Kalman controller presented in Sect. 2.2.2, when the SNR is reasonable at low frequencies and the turbulence evolution is standard. In other cases, which are extreme conditions, the model used in the Kalman filter can be improved to account for static components (see Eq. (28) and following). Additional computational cost is limited as we only use a diagonal matrix and filtering could also be limited to low order modes. Similar results have already been obtained for slowly varying aberrations, using exactly the same method. Study is still under progress.

5. VIBRATION FILTERING

5.1. Vibration Model and Kalman Filter Modification

Vibration filtering is an example of the adaptability of Kalman filter. Most of the ground-based telescopes must cope with vibrations. These vibrations can be due to motorization, driving of apparatus or to an excitation of mechanical eigen modes of the facilities by the wind. Integrator or OMGI are not able to filter them specifically and amplify them as soon as they are in the overshoot. Predictors can manage them as they use temporal priors as in.[25] The Kalman filter is also able to handle them, as suggested in[1] and we propose a solution to introduce pure vibration filtering. This solution has been simulated and results are analysed in Sect. 5.2. For simplification, we assume that each measured mode of the turbulence can be confronted to only one pure frequency vibration at most. For each mode, the frequency of vibration is supposed to be known. A typical example is a known vibration at frequency f_{vib} perturbing the system, but for which the effect on each mode is unknown. We should then filter this vibration on all modes. Thus the vibration can be described by a sinusoidal perturbation on any mode by $a(t) = A\cos(2\pi f_{vib} t + \varphi)$ where A, φ are the amplitude and phase of the perturbation. This first model is deterministic and simple but efficient as we will see. In a discrete-time model, we can use the following form:

$$a_n = A\cos(2\pi f_{vib} nT + \varphi), \tag{30}$$

where $T = 1/f_{ech}$ is still the sampling period (note that taking into account the CCD integration would not change the form of the discretized signal). It is readily shown that:

$$a_{n+2} = 2cos\left(\frac{2\pi f_{vib}}{f_{ech}}\right) a_{n+1} - a_n, \tag{31}$$

which defines the temporal dynamics of the vibration induced perturbation for any mode amplitude. Note that this relation does not make any assumption on the amplitude and the phase of the vibration. We only need to know the frequency.

As for the static aberrations filtering, we modify the state vector by introducing the vibration induced phase perturbation ϕ^{vib}:

$$\mathbf{X}_n = \begin{pmatrix} \phi^{vib}_{n+1} \\ \phi^{vib}_{n} \\ \phi^{tur}_{n+1} \\ \phi^{tot}_{n} \\ \phi^{tot}_{n-1} \\ \mathbf{u}_{n-1} \\ \mathbf{u}_{n-2} \end{pmatrix}, \tag{32}$$

where $\phi^{tot}_n = \phi^{tur}_n + \phi^{vib}_n$. In this case, we need two occurrences of the vibration induced phase perturbation because of the second order relation given in Eq. (31). The vibration induced phase verifies the Eq. (31) so that the new equations for this state-space model are:

$$\mathbf{X}_{n+1} = \begin{pmatrix} \mathbf{A_{vib}} & -\mathbf{Id} & 0 & 0 & 0 & 0 & 0 \\ \mathbf{Id} & 0 & 0 & 0 & 0 & 0 & 0 \\ 0 & 0 & \mathbf{A_{tur}} & 0 & 0 & 0 & 0 \\ \mathbf{Id} & 0 & \mathbf{Id} & 0 & 0 & 0 & 0 \\ 0 & 0 & 0 & \mathbf{Id} & 0 & 0 & 0 \\ 0 & 0 & 0 & 0 & 0 & 0 & 0 \\ 0 & 0 & 0 & 0 & 0 & \mathbf{Id} & 0 \end{pmatrix} \mathbf{X}_n + \begin{pmatrix} 0 \\ 0 \\ 0 \\ 0 \\ 0 \\ \mathbf{Id} \\ 0 \end{pmatrix} \mathbf{u}_n + \begin{pmatrix} 0 \\ 0 \\ \mathbf{Id} \\ 0 \\ 0 \\ 0 \\ 0 \end{pmatrix} v_{n+1}, \tag{33}$$

$$\mathbf{S}_n = \begin{pmatrix} 0 & 0 & 0 & 0 & \mathbf{D} & 0 & -\mathbf{DN} \end{pmatrix} \mathbf{X}_n + \mathbf{W}_n. \tag{34}$$

where $\mathbf{A_{vib}} = 2\,cos\left(\frac{2\,\pi\,f_{vib}}{f_{ech}}\right)\mathbf{Id}$. Matrices A, B and C are thus modified according to Eq. (33) and Eq. (34). Several frequencies can be applied to each mode.

Accounting for non pure harmonic vibrations is also possible thanks to a modification of Eq. (31), which is indeed rather basic. Tests are in progress.

5.2. Vibrations Filtering and performance

Vibration filtering has been tested thanks to the simulator implementing the previous modification: we assume that several vibrations exist on different modes and should be filtered. This simulation is based on a NAOS [†] case. We assume all the vibrations can be described as in Eq. (31).

The partial description of the vibrations undergone on NAOS, [26] and the parameters of the vibrations that have been actually added to the incoming turbulent phase in the simulation are presented in Tab. 1.

For instance, a 17Hz vibration of 10000 nm^2 energy is added to the input signal on Zernike mode 2 and we modify Kalman models to take into account a 17Hz vibration on this mode according to Eq. (33). The priors used in the filter are rather accurate in this case: we know which modes undergo a vibration and at which frequency. But amplitude and phase do not need to be described. Moreover, the other modes are not concerned by vibration filtering: a reduction of the vector size can be done to decrease the computation cost. As for the input, each modal vibration defined by its frequency, amplitude and an indifferent phase is added to the input phase in the form Eq. (30).

Figures 4 a) and b) illustrate the fact that the overall system behaves like a notch filter for each Zernike mode as for the vibrations induced phase perturbations. They are almost completely filtered, in a 1 Hz FWHM band. The gain in term

Zernike mode	frequency range (Hz)	Energy (min/max) in nm^2	filtered and simulated frequency	simulated Energy
2	16-18	3000/10000	17	10000
	48-55	2000/5000	–	–
	68-70	0/1000	–	–
3	16-18	3000/10000	17	10000
	48-55	2000/5000	–	–
	68-70	0/1000	–	–
4	42-48	500/1000	47	1000
5	32-34	200/500	33	500
6	32-34	200/500	33	500
9	41	200/400	41	400
	43-50	200/400	–	–
10	41	200/400	41	400
	43-50	200/400	–	–

Table 1. Description of NAOS measured vibrations and vibrations introduced in simulation

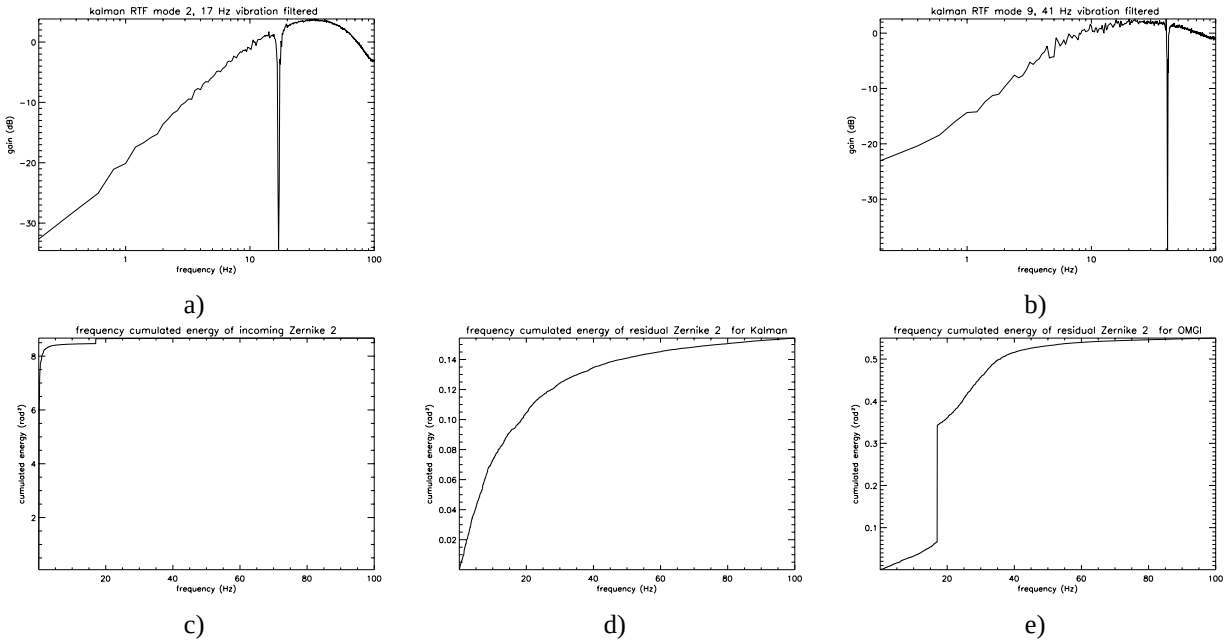

Figure 4. RTFs of the vibration filtering Kalman controller for the NAOS configuration of vibrations. Zernike modes 2 and 9 RTFs are presented on a) and b); result in term of frequency cumulated energy of Zernike mode 2 for input turbulence c), residual phase for Kalman filter d) and OMGI e).

of Strehl ratio is directly related to the presence of vibrations and their amplitude. Figures 4 c) and d) show the frequency cumulated energy of the input and residual phase. Usually, the vibration (represented by a step of energy in the plot) is not reduced. Here it is completely filtered. The consequence in term of Strehl Ratio is flagrant: in the conditions given in Sect. 2.3, and in presence of the vibrations described here before, the average OMGI Strehl Ratio is 20% over a 2000 short exposures images, and 43% for enhanced Kalman filter.

It is also possible for instance to filter a known vibration (for instance a 50 Hz vibration) on all modes *a priori*, not knowing on which ones the vibration will appear. As underlined before, the amplitude and phase of the vibration do not

[†]Nasmyth Adaptive Optics System

matter: we do not need more information on the vibration. That also means that any sudden change of phase or amplitude will be taken into account after a transitory period. A slow variation of amplitude and/or phase can also be managed as long as it does not represent a vibration frequency shift greater than the 1Hz FWHM.

Of course model and signal match, hence the final efficiency of our filter. The filtering of an unknown vibration defined around a known frequency needs enlarging the vibration bandwidth. This is another model refinement which is already under consideration. Computational cost is increased, but note once more that the matrix $\mathbf{A}_{\mathbf{vib}}$ is diagonal and providing the modes concerned by the vibrations are known, the global cost can be drastically reduced by filtering only a few modes.

6. CONCLUSION

Thus, the Kalman filter based control law provides an optimal closed-loop control for AO/MCAO systems, in terms of minimum mean square error. The classical principle of separation leads to considering to different problems, first a stochastic estimation of the turbulent phase, second a deterministic estimation of the best control. The Kalman filter and a standard projection on the DM modes basis offer the optimal solutions of these two problems. The Kalman filter approach also offers a global and formalized framework. We have here proposed a characterization of the Kalman filter in terms of frequential response and transfer matrix. A controller transfer matrix have been computed thanks to Kalman equations and the system Rejection Transfer Matrix have been deduced. It has been also shown that the matrix could be approximated by transfer functions, in the particular case of a simplified AO system. This approach gives much information about Kalman filter behavior particularly compared to other classical controller.

Additional perturbations have been considered such as static aberrations or slowly varying aberrations. They may not be well attenuated for very low SNR and all the more as the dynamics of the turbulent phase hardly account for these perturbations. A model improvement is however easily obtained to account for static aberrations and leads to a high quality filtering of these components. Vibration filtering has also been proposed and tested showing very good performance in a realistic case. Pure vibrations are estimated and attenuated on any mode. Of course the model used is rather simple and should be modified so as to account for larger bandwidth vibrations. All these improvements are done easily in the Kalman filter framework, using common methods.

Considering computational cost, estimation of gain matrix is done off-line, so without any further time delay. Although matrices sizes increase, most of the matrices are sparse, and static aberration or vibrations do not need to be filtered on all modes. We can then expect a huge reduction of computational cost.

As we only considered here a simplified AO system in which Zernike modes are measured and corrected directly, we now aim at introducing more realistic models. Real WFSs and DMs are to be considered, and the previous results and performance confirmed in these conditions. Extension to MCAO case will then be discussed. But we can already expect static aberrations and vibrations to be filtered a well, as it only depends on the incoming phase model.

ACKNOWLEDGMENTS

The first author received a PhD grant from DGA, Ministère de la Défense, France. Part of this study has been supported by EC contract RII3-CT-2004-001566. The authors thank B. Le Roux for fruitful discussions.

REFERENCES

1. B. Le Roux, J.-M. Conan, C. Kulcsár, H. F. Raynaud, L. M. Mugnier, and T. Fusco, "Optimal control law for multi-conjugate adaptive optics.," **4839**, PSPIE, SPIE, 2003.
2. B. Le Roux, J.-M. Conan, C. Kulcsár, H. F. Raynaud, L. M. Mugnier, and T. Fusco, "Optimal control law for classical and multiconjugate adaptive optics," *J. Opt. Soc. Am. A.* **21(7)**, pp. 1261–1276, 2004.
3. B. Le Roux, *Commande Optimale en Optique Adaptative Classique et Multiconjuguée*. PhD thesis, Université de Nice Sophia-Antipolis, 2003.
4. A. Tokovinin, M. Le Louarn, and M. Sarazin, "Isoplanatism in multi-conjugate adaptive optics system.," *J. Opt. Soc. Am. A* **17(10)**, pp. 1819–1827, 2000.
5. A. Knutsson and M. Owner-Petersen, "Emulation of dual-conjugate adaptive optics on an 8-m class telescope," *Optics Express* **11**(18), 2003.

6. M. Langlois, C. D. Saunter, C. N. Dunlop, R. M. Myers, and G. Love, "Multiconjugate adaptive optics: laboratory experience," *Optics Express* **12**(8), 2004.
7. B. Ellerbroek, F. Rigaut, C. Boyer, C. D'Orgeville, and M. Hunten, "MCAO for Gemini South," in *Adaptive Optical Systems Technologies II*, P. L. Wizinowich, ed., *Proc.SPIE* **4839-07**, 2002.
8. R. Ragazzoni, T. Herbst, W. Gaessler, D. Andersen, C. Arcidiacono, A. Baruffolo, H. Baumeister, P. Bizenberg, E. Diolaiti, S. Esposito, J. Farinato, H. Rix, R. Rohloff, R. Riccardi, P. Salineri, R. Soci, E. Vernet-Viard, and W. Xu, "A visible MCAO channel for Nirvana at LBT," in *Adaptive Optical Systems Technologies II*, P. L. Wizinowich, ed., *Proc.SPIE* **4839-65**, 2002.
9. E. Marchetti, N. Hubin, E. Fedrigo, R. Donaldson, R. Conan, M. Le Louarn, B. Delabre, F. Franza, D. Baade, C. Cavadore, A. Balestra, R. R. J.-L. Lizon, J. Farinato, E. Vernet-Viard, E. Diolaiti, D. Butler, S. Hippler, and A. Amorin, "MAD the ESO Multiconjugate Adaptive optics Demonstrator," in *Adaptive Optical Systems Technologies II*, P. L. Wizinowich, ed., *Proc.SPIE* **4839-38**, 2002.
10. B. Le Roux, R. Ragazzoni, R. Arcidiacono, J.-M. Conan, C. Kulcsár, and H. F. Raynaud, "Kalman filter based optimal control law for star oriented and layer oriented multiconjugate adaptive optics.," **4839**, PSPIE, SPIE, 2004.
11. R. Flicker, F. Rigaut, and B. Ellerbroek, "Comparison of multiconjugate adaptive optics configurations and control algorithms for the gemini-south 8-m telescope," in *Adaptive Optical Systems Technologies*, P. L. Wizinowich, ed., *Proc.SPIE* **4007**, 2000.
12. L. Gilles, B. Ellerbroek, and C. Vogel, "Layer-oriented multigrid wavefront reconstruction algorithms for multi-conjugate adaptive optics," in *Adaptive Optical Systems Technologies II*, P. L. Wizinowich, ed., *Proc.SPIE* **4839**, 2002.
13. B. Ellerbroek, L. Gilles, and C. Vogel, "A computationally efficient wavefront reconstructor for simulations of multi-conjugate adaptive optics on giant telescopes," in *Adaptive Optical Systems Technologies II*, P. L. Wizinowich, ed., *Proc.SPIE* **4839**, 2002.
14. F. Quiros-Pacheco, C. Petit, J. Conan, T. Fusco, and E. Marchetti, "Control law for the multi-conjugated adaptive optics demonstrator.," PSPIE, SPIE, 2004.
15. T. Fusco, *Correction partielle et anisoplanetisme en Optique Adaptative : traitements a posteriori et Optique Adaptative Multiconjuguée*. PhD thesis, Université de Nice Sophia-Antipolis, 2000.
16. E. Gendron and P. Lena, "Astronomical Adaptive optics I. modal control optimization," *Astronomy and Astrophysics* **291**, pp. 337–347, 1994.
17. E. Gendron and P. Lena, "Astronomical Adaptive Optics II. experimental results of an optimize modal control," *Astronomy and Astrophysics* **111**, pp. 153–167, 1994.
18. T. Fusco, J.-M. Conan, V. Michau, and G. Rousset, "Noise propagation for Multiconjugate Adaptive Optics systems," in *Optics in atmospheric Propagation and Adaptive Systems IV*, A. Kohnle, J. D. Gonglewski, and T. J. Schmugge, eds., **4538**, pp. 144–155, PSPIE, SPIE, (Bellingham, Washington), 2002.
19. R. Paschall and D. Anderson, "Linear Quadratic Gaussian control of a deformable mirror adaptive optics system with time-delayed measurements," *Applied Optics* **32**(31), pp. 6347–6358, 1993.
20. T. Fusco, J.-M. Conan, G. Rousset, L. Mugnier, and V. Michau, "Optimal wavefront reconstruction strategies for multiconjugate adaptive optics.," *J. Opt. Soc. Am. A* **18**, 2001.
21. D. Gavel and D. Wiberg, "Toward strehl-optimizing adaptive optics controllers," in *Adaptive Optical Systems Technologies II*, P. L. Wizinowich, ed., *Proc.SPIE* **4839-107**, 2002.
22. K. J. Aström, *Introduction to Stochastic Control Theory*, Academic Press, 1970.
23. H. V. Trees, *Detection, Estimation and Modulation Theory, Part I*, Wiley, New York, 1968.
24. E. Rigaut and E. Gendron, "Laser guide star in adaptive optics : the tilt determination problem," *Astron. Astrophys.* **261**, pp. 677–684, 1992.
25. C. Dessenne, *Commande modale et prédictive en optique adaptative classique*. PhD thesis, Université Paris VII, 1998.
26. D. Mouillet, T. Fusco, and G. Rousset, "Very large telescope nasmyth adaptive optics system test report," tech. rep., ONERA and ODP and LAOG, 2002.